Pulse Motor Control for Maximizing Average Velocity

Anthony J. Calise* and J. V. R. Prasad†
Georgia Institute of Technology, Atlanta, Georgia

This paper examines the problem of optimal pulse rocket motor control for minimum time to a specified final range. A complete characterization of the pulsing conditions is derived for the constant altitude case. The results are portrayed in the form of pulse-firing envelopes (one for each pulse) that are range- and velocity-dependent. For the variable altitude case, the problem of optimized guidance and pulse motor control in the vertical plane is treated. One of the major conclusions from this problem analysis is that the use of pulse motors offers little advantage when vertical plane guidance is optimized in the absence of constraints. Special attention is given to the optimality conditions that arise at the junction of boost and coast arcs, and a numerical procedure for computing the junction condition is outlined.

Introduction

INTEREST in optimal pulse control arises from developments in pulsed solid rocket motor technology for tactical missile applications. These motors have varying degrees of in-flight propulsion capability. The most promising candidates from a cost and reliability viewpoint are multiple pulse motors with variable pulse initiation times, and they offer the potential for significant range improvement for a given total impulse. Earlier papers that have addressed the optimal control of pulsed rocket motors have either used numerical optimization techniques[1-3] or have formulated the problem in the context of the calculus of variations.[4,5] When using the calculus of variations, the necessary conditions of optimal pulse control appear in a nonstandard form due to the fact that only the pulse initiation time is controllable, whereas the pulse duration is fixed by the motor design.[5] These studies have concentrated primarily on the problem of maximizing range for a specified terminal velocity or maximizing terminal velocity for a specified range. In this paper, we examine the problem of minimizing time (maximizing average velocity) for a specified range, using the necessary conditions as derived in Ref. 5. The results are related at the point of maximum range where the minimum time, maximum terminal velocity, and maximum range solutions reduce to the same pulsing condition.

Two separate problem formulations are considered. The first is for flight at constant altitude, where a complete characterization of the pulsing conditions is derived, and the results are portrayed in the form of pulse-firing envelopes (one for each pulse) that are range- and velocity-dependent. The second formulation considers an air-to-surface or surface-to-surface application, in which the problem is to simultaneously optimize the vertical plane guidance and the pulse motor control. One major conclusion from the results of this analysis is that the multiple pulse motor offers little advantage when the vertical plane guidance is optimized in the absence of constraints. Numerical results are presented for a typical surface-to-surface missile.

Received June 8, 1987; revision received Oct. 8, 1987.

*Professor, Aerospace Engineering. Senior Member AIAA.
†Research Engineer, Aerospace Engineering.

Optimal Pulse Control for Maximizing Average Velocity

In this section, we consider the problem of optimal pulse control to reach a specified range in minimum time, with a constraint on minimum terminal velocity. This is the same as maximizing average velocity. The dynamics are confined to constant altitude flight, where the equations of motion can be simplified to

$$\mathrm{d}x/\mathrm{d}t = V, \qquad x(0) = 0,\ x(t_f) = x_f \tag{1}$$

$$\mathrm{d}E/\mathrm{d}t = (T - D)V/W, \qquad E(0) = E_0 = h_0 + V_0^2/2g \tag{2}$$

$$\mathrm{d}m/\mathrm{d}t = -cT, \qquad m(0) = m_0 \tag{3}$$

The Hamiltonian for this system is

$$H = \lambda_x V + \lambda_E(T\text{-}D)V/W - \lambda_m cT + 1 \tag{4}$$

and the co-state variables satisfy

$$\dot{\lambda}_x = 0, \qquad \lambda_x(t_f) - \text{free} \tag{5}$$

$$\dot{\lambda}_E = -\partial H/\partial E, \qquad \lambda_E(t_f) = 0 \quad \text{when} \quad V_f > V_{\min} \tag{6}$$

$$\dot{\lambda}_m = -\partial H/\partial m, \qquad \lambda_m(t_f) = 0 \tag{7}$$

where $V_{\min}$ is the minimum terminal velocity and V_f the final velocity when $V_f \geq V_{\min}$. When $V_f < V_{\min}$, the final velocity is $V_{\min}$ and V_f is used only as a variable parameter. If we evaluate (4) at $t = t_f$ and use the fact that λ_x is constant, it follows that

$$\lambda_x(t) = -1/V_f, \qquad V_f > V_{\min} \tag{8}$$

Since only the pulse initiation time is controlled, the first-order necessary conditions for optimality take on a nonstandard form[5]

$$H_T(t_i) = H_T(t_i + \Delta_i) \tag{9}$$

$$H^0(t_i) = H^0(t_i + \Delta_i) = 0 \tag{10}$$

where $H_T = \partial H/\partial T$, $H^0 = H(T = 0)$, *and* t_i, Δ_i are the pulsing time and pulse duration for the ith pulse. Condition (10) requires the added assumption that the trajectory ends in a coasting arc.

The pulsing condition is first derived assuming constant mass and later corrected for mass variations. For the constant mass case, the third term in (4) is ignored, and conditions (9) and (10) result in

$$\lambda_E V/W|_{t_i} = \lambda_E V/W|_{t_i+\Delta_i} \tag{11}$$

$$(\lambda_x V - \lambda_E DV/W + 1)|_{t_i} = (\lambda_x V - \lambda_E DV/W + 1)|_{t_i+\Delta_i} = 0 \tag{12}$$

Combining (8) with (11, 12), we have

$$(V - V_f)/D|_{t_i} = (V - V_f)/D|_{t_i+\Delta_i} \tag{13}$$

Following the analysis in Ref. 5, correction for mass variation results in

$$(V_f - V)/D|_{t_i} = C_m^i (V - V_f)/D|_{t_i+\Delta_i} \tag{14}$$

where

$$C_m^i = (1 - a_i^+ L_i)/(1 + a_i L_i) \tag{15a}$$

$$a_i^+ = [(T_i - D)/2T_i]_{t_i+\Delta_i} \tag{15b}$$

$$a_i = [(T_i - D)/2T_i]_{t_i} \tag{15c}$$

$$L_i = \ell n[m_i/(m_i - \Delta m_i)] \tag{15d}$$

For $T_i \gg D, C_m^i$ can be approximated by

$$C_m^i = (1 - 0.5L_i)/(1 + 0.5L_i) \tag{16}$$

In (15d), m_i is the mass at $t = t_i$ and Δm_i is the propellant mass in the ith pulse.

Use of the pulsing condition in (14) requires knowledge of $V_f(R)$ where R is the range to go. This functional relation can be established numerically by generating a one-parameter family of optimal trajectories. That is, pick V_f and integrate forward in time using (14) as the pulsing condition. The trajectory is terminated when all the pulses are fired and $V = V_f$. If $V_f < V_{\min}$ (the minimum terminal velocity constraint), then the trajectory is terminated when $V = V_{\min}$. Under this condition, V_f is still used to parameterize the pulsing condition (13), but no longer corresponds to the terminal velocity. It simply represents the unknown value of λ_x. Note that range and time are a byproduct of this integration procedure, and we can say that any other pulsing law will result in a greater flight time (lower average velocity for this range).

For a numerical illustration, consider a simple parabolic drag polar model

$$D = qSC_{D_0} + KL^2/qS, \qquad L = W \tag{17}$$

with $S = 0.9$ ft^2, $C_{D_0} = 0.3$, $K = 0.3$, and $W = 500$ lb. Figure 1 illustrates the operation of the pulse-firing condition in (13) for several values of V_f at an altitude of 30,000 ft. If the terminal velocity was left unconstrained, the optimal terminal velocity corresponds to the point where the ratio in (13) first becomes positive. The highest curve in Fig. 1 corresponds to the curve obtained for maximizing terminal velocity in Ref. 5. In the context of minimizing time, it would be used to achieve the greatest possible range. Note that the stopping condition would be $V(t_f) = 0$. Thus, without a constraint on minimum terminal velocity, this curve and several of the lower curves would not make sense. If, on the other hand, we specify, for example, that $V(t_f) > 1500$ ft/s, then all of the curves can be used. The trajectories using $V_f > 1500$ would terminate at $V = V_f$, whereas the trajectories using $V_f < 1500$ would terminate at $V = 1500$.

There is a condition that prevents the curves for large values of V_f from being used. This corresponds to the situation in which the peak in the curve falls beyond the thrust = drag line indicated in the figure. For this situation, it is not possible for the missile to accelerate to satisfy the equality condition in (13). Note that the ΔV indicated in Fig. 1 for $V_f = 500$ depends on the pulse magnitude and duration, and decreases for increasing values of V_f due to the increasing drag as velocity increases. It approaches 0 as V_f approaches 2500 for the pulse motor parameter values given in Fig. 2.

Figure 2 illustrates a performance curve that was generated for a two-pulse motor using the procedure just described. The parameters for the study are $V_0 = 3500$ ft/s, $V_{\min} = 1500$ ft/s, $h = 30{,}000$ ft, and two pulses were controlled by the condition in (13). The points on the curve correspond to different values of V_f ranging between 0 and 2500. The missile's starting weight is 500 lb. The indicated times are minimum times for the corresponding ranges. With the information from the runs, one can construct the pulse-firing envelopes shown in Fig. 3, which show the velocity and range-to-go combinations at which each pulse should be fired. What is interesting here is that these envelopes are independent of starting velocity. Two typical members from the family of optimal trajectories used to generate the envelopes are also shown. The V vs range-to-go profile for $V_f = 1000$ represents a typical profile in which both pulses are internal to the trajectory and separated in time. Note that the firing velocity for the second pulse is slightly lower due to mass variation and that the trajectory is terminated at $V = V_{\min}$. In general, there would be little correlation between the pulse-firing velocities for the case of unequal pulses. For high initial velocity and short ranges, we encounter the $T = D$ condition illustrated in Fig. 1. Under these circumstances, we fire at the peak of the $(V - V_f)/D$ curve corresponding to $V_f = 2500$ and remain there, which causes the second pulse to immediately follow the first pulse. This is also illustrated in Fig. 3 for $V_f = 2500$. Note that under these conditions we are still satisfying the pulse-firing condition in (13).

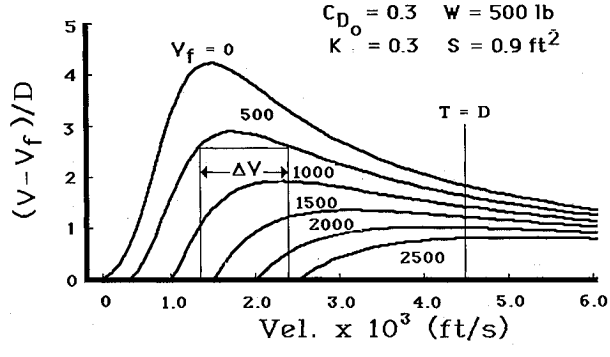

Fig. 1 Pulse-firing equation for several values of V_f.

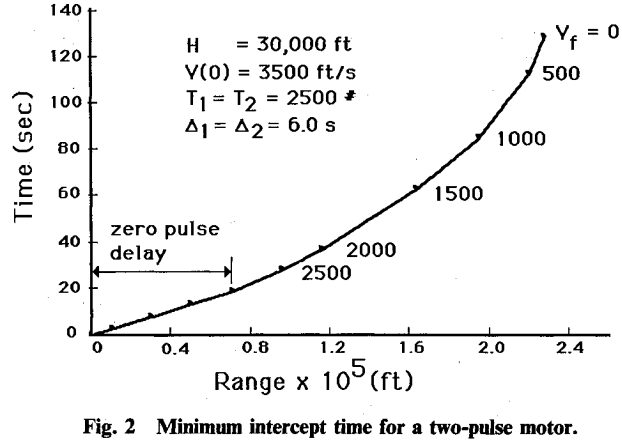

Fig. 2 Minimum intercept time for a two-pulse motor.

Other unusual cases can arise. For example, if the initial velocity and range to go lie within the envelope of Fig. 3 for the first pulse, then we would immediately fire the first pulse. Likewise, if the initial velocity is high and the range to go is small, then we fire both pulses sequentially either when the velocity decreases to 4500 ft/s or when the time to go is less than the total pulse duration time (depending on which occurs first). In the latter case, we would not wait for an intersection with the pulse-firing envelope to occur. From this discussion, it can be seen that we have a complete characterization of optimal pulse utilization for minimum time to a specified range.

Vertical Plane Optimal Guidance and Pulse Control

This section treats the problem of optimal guidance simultaneous with optimal pulse motor control. It is shown that, in the absence of constraints along the trajectory, there is little advantage to having a pulsed motor when the objective is to maximize average velocity. The optimal guidance analysis identifies two flight profiles that should be flown, one during boost and one during glide. The boost profile is independent of the total range to be flown. The analysis is for a constant mass missile, but with the mass updated during the boost phase.

The following two-state model has been used in aircraft analysis for vertical plane optimization:

$$\dot{x} = V \tag{18}$$

$$\dot{E} = (T - D)V/W \tag{19}$$

where the dynamics are approximated for level flight conditions ($\gamma = 0$, $L = W$). The optimal flight profile is derived by treating altitude as a control variable.[6,7] For the case of constant thrust and minimum time to a specified final range, the Hamiltonian is

$$H = \lambda_x V + \lambda_E (T - D)V/W + 1 = 0 \tag{20}$$

where the co-state variables satisfy (5, 6). From Appendix A, it follows that in the absence of constraints

$$h^*(E) = \arg\max_h [(T - D)V/(\lambda_x V + 1)]\big|_{E=\text{const.}} \tag{21}$$

where it must be recognized in (21) that wherever V appears, it is replaced by

$$V = [2g(E - h)]^{\frac{1}{2}} \tag{22}$$

Now, the condition for optimal pulsing in the constant altitude case is given by (13). To examine the variable altitude case, we define the altitude profile by (21). It was found that the ratio $(V^* - V_f)/D^*$ was a monotonic increasing function of E, where V^* and D^* are the values corresponding to $h = h^*$. Thus, during a boost, the condition in (13) can never be encountered when the altitude profile is optimized. Therefore, in the analysis that follows, it is assumed that all the pulses are fired as early as possible. This assumption degenerates the pulse motor problem into a boost-coast problem.

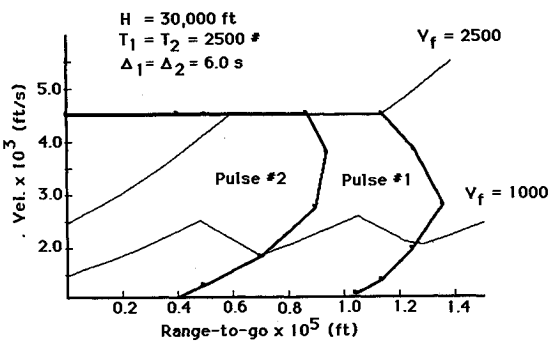

Fig. 3 Pulse-firing envelopes.

Coast Solution

Since the trajectory ends in a coasting arc and $H(t_f) = 0$ and is constant during a coasting arc, it follows that

$$H_c = \lambda_x V - \lambda_E DV/W + 1 = 0 \tag{23}$$

$$\partial H_c/\partial h = 0 \tag{24}$$

are the necessary conditions for optimality. If we let $\lambda_x = -1/V_f$ be a parameter in the optimization (as was done in the constant altitude case), then (21, 22) represent two equations for the two unknowns, λ_E and h. Using the general approach outlined in Appendix A for solving equations of this form, we have that the optimal altitude profile and co-state λ_E during coast are defined by

$$h_c(E) = \arg\max_h [DV/(\lambda_x V + 1)]\big|_{E=\text{const.}} \tag{25}$$

$$\lambda_E^c(E) = W(\lambda_x V_c + 1)/D_c V_c \tag{26}$$

where V_c and D_c are the values corresponding to h_c at current E, and D_c is also computed for lift = coast weight. This defines a family of descent paths parameterized by V_f. A typical family generated using the aerodynamic model of Appendix B is illustrated in Fig. 4.

Boost Solution

The Hamiltonian during boost is given by

$$H_B = \lambda_x V + \lambda_E (T - D)V/W + 1 = C \tag{27}$$

It is constant, but not equal to zero. The constant value C is due to the discontinuity in $\dot{E}$ that occurs at the junction of the boost and coast arcs.[8] At this junction, there will also be, in general, a discontinuity in the optimal altitude profile and, consequently, a discontinuity in V since the optimization of h is performed at a constant E. However, λ_E remains continuous at the junction. Again, if we use the general approach outlined in Appendix A, the optimal altitude profile and co-state during boost are

$$h_B(E) = \arg\max_h [(T - D)V/(\lambda_x V + 1 - C)]\big|_{E=\text{const.}} \tag{28}$$

$$\lambda_E^B(E) = -W(\lambda_x V_B + 1 - C)/(T - D_B)V_B \tag{29}$$

where V_B and D_B are the values corresponding to h_B at the current E, and D_B is computed for lift = current weight.

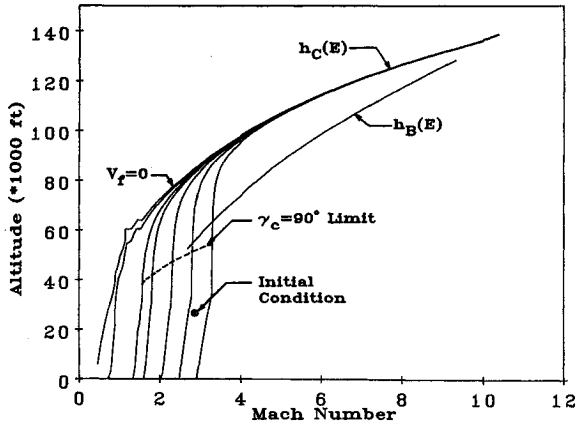

Fig. 4 Boost and coast trajectories for several values of V_f = 0, 600, 1200, 1500, 2000, 2500, and 3000 ft/s (left to right).

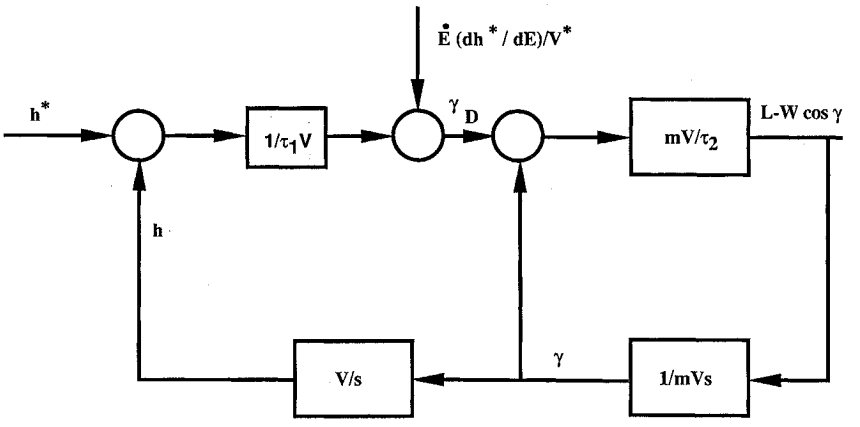

Fig. 5 Proportional vertical lift calculations.

Matching Boost and Coast Arcs

Condition (28) establishes the optimal profile to be flown during boost. However, the Hamiltonian value C must be first determined based on the condition that λ_E is continuous at the junction. Let $\bar{E}$ denote the energy where the two arcs are joined. If we assume $\bar{E}$ is known for the moment, then $h_c(\bar{E})$ and $V_c(\bar{E})$ are determined using (25). An initial guess for C follows if we assume $h_B(\bar{E}) = h_c(\bar{E})$. Comparing (23) and (27), we have

$$C_0 = T(\lambda_x V_c + 1)/D_c|_{\bar{E}} \tag{30}$$

Then, the following steps can be executed to determine C for a given E:

1) Pick C_0, set $i = 0$.
2) Calculate $h_B(\bar{E})$ for $C = C_i$.
3) Use (26) and (29) and the continuity of λ_E at $\bar{E}$ to calculate a new value for C_i. $C_{i+1} = (T - D_B)(\lambda_x V_c + 1)V_B/D_c V_c + \lambda_x V_B - 1$.
4) If converged on $h_B(\bar{E})$, stop; otherwise, set $i = i + 1$ and return to step 2.

The preceding procedure assumes $\bar{E}$ is known. To determine $\bar{E}$, Eqs. (2) and (3) are integrated forward in time using Eq. (28) to define the altitude profile for a presumed value of C. Thus, a second iteration is required that uses the iteration for C as an inner loop:

1) Pick $\bar{E}_0$, set $j = 0$.
2) Calculate $C(\bar{E}_j)$ – inner loop iteration.
3) Integrate Eqs. (2) and (3) over the total boost phase using Eq. (28) to define the altitude profile. This determines $\bar{E}_{j+1}$.
4) If you have converged on $\bar{E}$, then stop, otherwise set $j = j + 1$ and return to step 2.

A typical boost profile is illustrated in Fig. 4 for the aerodynamic and propulsion model of Appendix B. It was found that the parameter V_f had no perceptible effect on the solution. This fact has a significant practical implication in that only the coast phase is dependent on range-to-go.

A portion of the descent paths for $V_f > 1200$ ft/s and below the dashed line in Fig. 4 cannot be flown physically. The point where this occurs can be determined by examining the flight-path angle required to just maintain the path. We have the following relations that exist along the descent path:

$$\dot{h}_c = V_c \sin\gamma_c = (\mathrm{d}h_c/\mathrm{d}E)\dot{E}_c \tag{31}$$

$$\dot{E}_c = -D_c V_c/W \tag{32}$$

Thus,

$$\gamma_c = -\sin^{-1}[(\mathrm{d}h_c/\mathrm{d}E)D_c/W] > \gamma_{\min} \tag{33}$$

The dashed line in Fig. 4 corresponds to the point at which the argument in (33) becomes greater than one.

Enforcing Path Constraints

It is possible to enforce certain path constraints as part of the process of generating the boost and coast profiles. An altitude-step search procedure is used to find the maximum of the functions in (25) and (28). At each step, the angle of attack (for lift = weight) and dynamic pressure are computed. Limits for $\alpha_{\max}$ and $q_{\min}$ can be used to bound the search at high altitude. These limits were not enforced for any of the paths in Fig. 4. A low-altitude limit could be established based on a temperature-limit boundary; however, the slope of these boundaries are normally such that they cannot be flown during boost. In this case, it is necessary to delay the pulses. Therefore, this constraint was not enforced in the altitude search.

In order to achieve a desired terminal flight-path angle, it is necessary to impose a minimum flight-path angle constraint in the search procedure for the coast solution of (25). Since the constraint is encountered near the end of the coasting arc, profiles with a flight-path angle constraint could easily be generated for increasing energy, wherein an increase in altitude for a given ΔE is limited to satisfy a prescribed limit in accordance with (33). However, no constraint on terminal flight-path angle was imposed in this study.

Proportional Vertical Lift Calculation

Equations (25) and (28) define the optimal coast and boost altitude profiles. For simulation purposes, it is necessary to define a guidance law that will control the missile so that these profiles are followed. A simple proportional control law used to define lift in the vertical plane is derived in this section.

We first define a desired flight-path angle as

$$\gamma_D = (h^* - h)/\tau_1 V + \dot{E}(\mathrm{d}h^*/\mathrm{d}E)/V^* \tag{34}$$

where h^* denotes the desired altitude (h_c or h_B) and V^* is the corresponding velocity at the current E. The second term is an approximation to the flight-path angle needed to maintain the desired path. Lift is computed based on the desired flight-path angle rate proportional to $(\gamma_D - \gamma)$

$$\dot{\gamma}_D = (\gamma_D - \gamma)/\tau_2 = (L - W\cos\gamma)/mV \tag{35}$$

Solving for L, we have

$$L = mV(\gamma_D - \gamma)\tau_2 + W\cos\gamma \tag{36}$$

A block diagram of these calculations is given in Fig. 5. For constant V, the characteristic equation for this guidance loop is

$$\tau_1\tau_2 s^2 + \tau_1 s + 1 = 0 \tag{37}$$

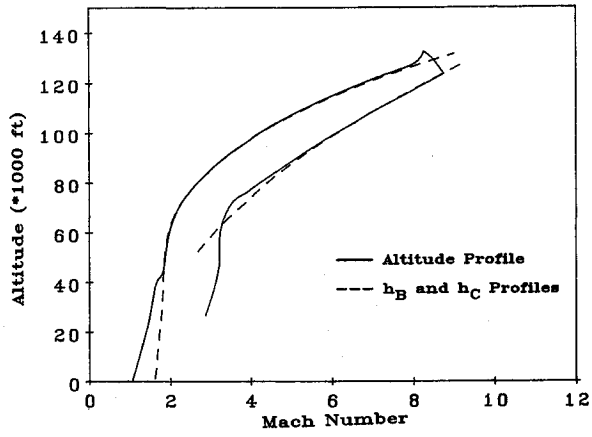

Fig. 6 Altitude vs Mach for $V_f = 1500$ ft/s.

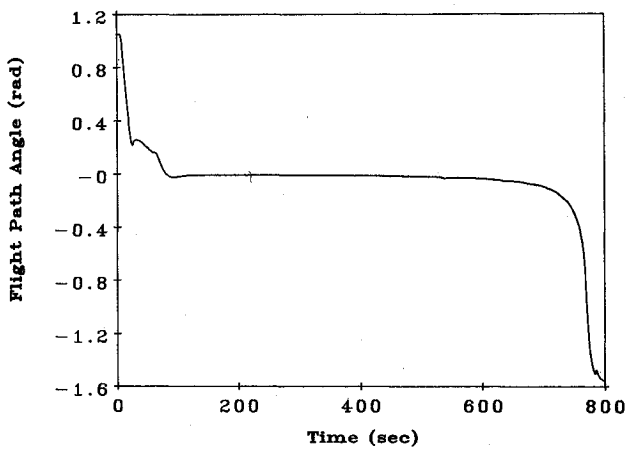

Fig. 7 Flight-path angle history for $V_f = 1500$ ft/s.

The natural frequency (ω) and damping ration (ζ) for this system are

$$\omega = 1/(\tau_1\tau_2)^{\frac{1}{2}} \tag{38}$$

$$\zeta = (\tau_1/\tau_2)^{\frac{1}{2}}/2 \tag{39}$$

It was found to be more convenient to specify the guidance parameters in terms of ω and ζ, and to then compute τ_1 and τ_2 for use in (34) and (36). The simulation permits a set of values for both boost and coast phases of flight.

Numerical Results

This section details the simulation results obtained for a long-range surface-to-surface point mass missile model. The simulation was done for a five-state model for x, h, V, γ and W dynamics. The aerodynamic, weight, and propulsion data are summarized in Appendix B.

The initial conditions were taken to be second-stage takeover conditions for the missile that were defined as

altitude = 26,667 ft
velocity = 2900 ft/s
flight-path angle = 59.7 deg

The missile was considered to be in the boost phase from the start, and both pulses were fired one after the other. The simulation was terminated when the missile reached an altitude of 600 ft.

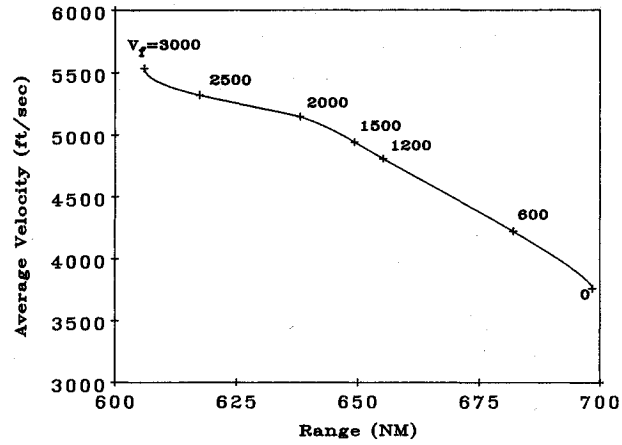

Fig. 8 Average velocity vs range.

Figure 6 illustrates the flight profile for $V_f = 1500$ ft/s. Also shown are the corresponding optimal boost and coast altitude profiles. The simple proportional guidance law tracks the optimal profiles with little difficulty, except near the end of the trajectory, where the optimal profile cannot be flown. The corresponding flight-path angle (γ) history is given in Fig. 7. The effect of range on average velocity was investigated by repeating the simulation for different values of V_f. This causes the guidance law to use the various coast profiles of Fig. 4. The results are summarized in Fig. 8, where it can be seen that range is improved as V_f is decreased, but at a significant cost in flight time.

Conclusions

This study has examined the problem of optimal pulse utilization for maximizing average velocity to a specified downrange. Two problems have been analyzed. The first problem considers constant altitude flight. A complete characterization of the pulsing conditions was derived, and the results can be portrayed in the form of pulse-firing envelopes (one for each pulse) that are range-to-go and velocity-dependent. These results are useful when mission constraints require that a portion of the trajectory be flown at constant altitude. The second problem addresses simultaneous optimization of the flight profile and pulse utilization. Pulsed motors offer little advantage when guidance is optimized in the absence of constraints. It was also found that standard energy-state approximations ($\gamma = 0$, $L = W$) do not apply well when flying to a low altitude with high terminal velocity.

Appendix A

This appendix documents a method for minimizing a Hamiltonian function with one unknown costate.

Given the Hamiltonian function

$$H(u) = f(u) + \lambda g(u) = 0 \tag{A1}$$

the sufficient conditions for the existence of a minimum for (A1) are

$$\partial H/\partial u = f_u + \lambda g_u = 0 \tag{A2}$$

$$\partial^2 H/\partial u^2 = f_{uu} + \lambda g_{uu} > 0 \tag{A3}$$

In a free-time problem where t does not explicitly appear in H, is is also necessary that $H = 0$. If we use (A1), this leads to

$$\lambda = -f/g, \qquad g \neq 0 \tag{A4}$$

Using (A4) in (A2) and (A3), we obtain

$$\partial H/\partial u = f_u - (f/g)g_u = 0 \tag{A5}$$

$$\partial^2 H/\partial u^2 = f_{uu} - (f/g)g_{uu} > 0 \tag{A6}$$

Define the function

$$L = g/f \tag{A7}$$

Taking the first and second partials yields

$$\partial L/\partial u = (fg_u - gf_u)/f^2 \tag{A8}$$

$$\partial^2 L/\partial u^2 = (fg_{uu} - gf_{uu})/f^2 - 2f_u(\partial L/\partial u)/f \tag{A9}$$

Setting (A8) equal to zero gives the same condition as in (A2) and (A4). Condition (A6) can be rewritten

$$\begin{aligned} gf_{uu} - fg_{uu} > 0, \quad & g > 0 \\ gf_{uu} - fg_{uu} < 0, \quad & g < 0 \end{aligned} \tag{A10}$$

By using $\partial L/\partial u = 0$ in (A9), it can be seen that the following will be equivalent to (A10):

$$\begin{aligned} \partial^2 L/\partial u^2 < 0, \quad & g > 0 \\ \partial^2 L/\partial u^2 > 0, \quad & g < 0 \end{aligned} \tag{A11}$$

From the foregoing, we can conclude that

$$\begin{aligned} \max\{L\}, \quad & g > 0 \\ \min\{L\}, \quad & g < 0 \end{aligned} \tag{A12}$$

is equivalent to the conditions in (A1–A3).

Appendix B

This appendix summarizes the aerodynamic and weight data of an advanced surface-to-air missile used in this study.

Some of the other parameters of the missile model are

$S_{ref} = 2.4$ ft^2 $\quad W_0 = 2135$ lbs

Pulse 1	*Pulse* 2
Thrust = 5500 lb	Thrust = 5500 lb
Pulse width = 32.6 s	Pulse width = 32.6 s
Pulse weight = 666 lb	Pulse weight = 666 lb

Table B1 Aerodynamic data

Mach no.	$C_{n\alpha}$/deg	C_{Ao} Boost	C_{Ao} Coast
0.01	0.141	0.243	0.260
0.20	0.141	0.243	0.261
0.60	0.145	0.225	0.243
0.80	0.155	0.219	0.236
0.90	0.161	0.215	0.232
0.95	0.167	0.237	0.255
1.05	0.190	0.292	0.319
1.15	0.190	0.306	0.331
1.25	0.162	0.313	0.337
1.50	0.143	0.349	0.371
2.00	0.134	0.314	0.333
2.50	0.127	0.273	0.288
3.00	0.127	0.241	0.253
4.00	0.130	0.201	0.209
10.00	0.108	0.129	0.131

Acknowledgment

This research was supported by the McDonnell Douglas Astronautics Company, St. Louis Division, under contract WS-PROP-1914.

References

[1]Glasson, D. P. and Mealy, G. L., "Optimal Guidance for Beyond Visual Range Missiles," The Analytic Sciences Corp., TR-3819, Reading, MA, July 1983.

[2]Cheng, V. H. L., Menon, P. K. A., Gupta, N. K., and Briggs, M. M., "Reduced-Order Approach to Near-Optimal Real-Time Pulse-Motor Ignition Control," AIAA Paper 85-0500, Jan. 1985.

[3]Menon, P. K. A., Cheng, V. H. L., Lin, C. A., and Briggs, M. M., "High Performance Missile Synthesis with Trajectory and Propulsion System Optimization," AIAA Paper 85–1956, CO, Aug. 1985.

[4]Calise, A. J. and Smith, S., "Optimal Pulse Motor Control," *Optimal Control Applications and Methods*, Vol. 4, Oct.–Dec., 1983, pp. 325–334.

[5]Calise, A. J. and Nagy, J., "Necessary Conditions for Optimal Pulse Control," *Journal of Guidance, Control, and Dynamics*, Vol. 9, Jan.–Feb., 1986, pp. 53–57.

[6]Bryson, A. E., Desai, M. N., and Hoffman, W. C., "Energy-State Approximation in Performance Optimization of Supersonic Aircraft," *Journal of Aircraft*, Vol. 6, Nov.–Dec., 1968, pp. 481–488.

[7]Calise, A. J., "Extended Energy Management Methods for Flight Performance Optimization," *AIAA Journal*, Vol. 15, March 1977, pp. 314–321.

[8]Bryson, A. E. and Ho, Y. C., *Applied Optimal Control,* Hemisphere, New York, 1975.